

# Mechanistic Studies of Diastereomeric Nickel(II) *N*-Glycoside Complexes Using Tandem Mass Spectrometry

Glenn Smith and Julie A. Leary\*

Contribution from the Department of Chemistry, University of California, Berkeley, California 94720

Received April 27, 1998

**Abstract:** Ni(II) *N*-glycoside complexes of four diastereomeric monosaccharides were synthesized and analyzed by fast atom bombardment-mass spectrometry. The average kinetic energy release (KER) associated with the formation of a C<sub>2</sub>H<sub>4</sub>O<sub>2</sub> neutral loss was indicative of stereochemical differences in the coordinated monosaccharide. Isotopic labeling studies and various linked scanning techniques were undertaken, suggesting multiple dissociation pathways from different reacting configurations, leading to the formation of isomeric [M-C<sub>2</sub>H<sub>4</sub>O<sub>2</sub>] product ions. Additionally, computational studies predict the presence of large structural differences between complexes possessing axial or equatorial C-2 substituents.

## Introduction

Increasing attention has been paid to the development of mass spectrometric techniques (MS) capable of analyzing the structures of carbohydrates.<sup>1</sup> The sensitivity available with MS is typically much greater than with conventional methods such as NMR spectroscopy or traditional chemical analyses<sup>2</sup>. Additionally, tandem MS experiments can be used to analyze the heterogeneous mixtures<sup>3</sup> often encountered with real biological samples, thereby greatly reducing the purity constraints associated with other analytical techniques. Many references can be cited which explore the problem of determining the number of monosaccharide units and/or ring substituents within a larger polysaccharide.<sup>1,4</sup> However, complete structural analysis of carbohydrates requires the further characterization of features depending upon subtle stereochemical variations. For instance, determination of the linkage position of a glycosidic bond requires the differentiation of structural isomers. Complete characterization of a carbohydrate also involves the identification of the individual monosaccharide units (e.g., D-glucose vs D-mannose, etc.) as well as the glycosidic linkage configuration ( $\alpha$  vs  $\beta$ ).

Success has been achieved in the analysis of metal/carbohydrate complexes using MS, particularly in characterizing stereochemical features of carbohydrates. Several papers have

detailed the use of alkali and alkaline earth adducts in differentiating the various linkage positions.<sup>5</sup> Fewer examples exist where the glycosidic bond configuration<sup>6</sup> or the monosaccharide units<sup>7,8</sup> are identified. Additionally, in previous studies we have shown that the dissociations of transition metal/*N*-glycoside complexes were sensitive to the stereochemical features present among a series of diastereomeric monosaccharides.<sup>8</sup> In one specific case,<sup>8a</sup> the kinetic energy release (KER) associated with the dissociation of FAB-generated Ni(II) *N*-glycoside complexes was shown to be indicative of the stereochemistry of a specific carbon center of the monosaccharide. However, there have been few detailed mechanistic studies of the dissociation of these types of metal/carbohydrate complexes.<sup>5b</sup> The present work will investigate the dissociation mechanisms of the previously reported series of Ni(II) *N*-glycoside complexes using various MS/MS techniques, isotopic labeling experiments, and computational studies.

## Experimental Section

**Instrumentation.** Fast atom bombardment ionization mass spectrometry (FAB-MS) was performed using a ZAB2-EQ mass spectrometer (Fisons/VG Analytical, Manchester, U.K.) of BEQ geometry. (o is an rf-only octapole collision cell fabricated in our laboratory<sup>9</sup> and replaces the conventional quadrupole in this particular instrument.) This instrument is equipped with three reaction regions.

The FAB-MIKES studies were carried out in the second reaction region between the magnet (B) and the electric sector (ESA). Spectra

\* To whom correspondence should be addressed. Telephone: (510)-643-6499. Fax: (510)-642-9295. E-mail: leary@garnet.berkeley.edu.

(1) (a) Reinhold: V. N.; Carr, S. A. *Mass Spectrom. Rev.* **1983**, 2, 153. (b) Egge, H.; Peter-Katalinic, J. *Mass Spectrom. Rev.* **1987**, 6, 331. (c) Egge, H.; Peter-Katalinic, J.; Karas, M.; Stahl, B. *Pure Appl. Chem.* **1991**, 63, 491. (d) Richter, W. J.; Müller, D. R.; Domon, B. *Methods Enzymol.* **1990**, 193, 607. (e) Gillette-Castro, B. L.; Burlingame, A. L. *Methods Enzymol.* **1990**, 193, 689. (f) Harvey, D. J. *J. Chromatogr. A* **1996**, 720, 429.

(2) Chaplin, M. F., Kennedy, J. F., Eds. *Carbohydrate Analysis: A Practical Approach*, 2nd ed.; Oxford University Press: New York, 1994.

(3) Busch, K. L.; Glish, G. L.; McLuckey, S. A. *Mass Spectrometry/ Mass Spectrometry: Techniques and Applications of Tandem Mass Spectrometry*; VCH Publishers: New York, 1988.

(4) (a) Linscheid, M.; D'Angona, J.; Burlingame, A. L.; Dell, A.; Ballou, C. E. *Proc. Natl. Acad. Sci.* **1981**, 78, 1471. (b) Carr, S. A.; Reinhold, V. N. *J. Carbohydr. Chem.* **1984**, 3, 381. (c) Reinhold: V. N.; Carr, S. A.; Green, B. N.; Petitou, M.; Choay, J.; Sinay, P. *Carbohydr. Res.* **1987**, 161, 305. (d) Mallis, L. M.; Wang, H. M. Loganathan, D.; Linhardt, R. J. *Anal. Chem.* **1989**, 61, 1453.

(5) (a) Zhou, Z.; Ogden, S.; Leary, J. A. *J. Org. Chem.* **1990**, 55, 5444. (b) Hofmeister, G. E.; Zhou, Z.; Leary, J. A. *J. Am. Chem. Soc.* **1991**, 113, 5964. (c) Staempfli, A.; Zhou, Z.; Leary, J. A. *J. Org. Chem.* **1992**, 57, 3590. (d) Fura, A.; Leary, J. A. *Anal. Chem.* **1993**, 65, 2805. (e) Lemoine, J.; Fournet, B.; Despeyroux, D.; Jennings, K. R.; Rosenberg, R.; de Hoffman, E. *J. Am. Soc. Mass Spectrom.* **1993**, 4, 197. (f) Dongré, A. R.; Wysocki, V. H. *Org. Mass Spectrom.* **1994**, 29, 700. (g) Reinhold: B. B.; Chan, S.-Y.; Chan, S.; Reinhold: B. B. *Org. Mass Spectrom.* **1994**, 29, 736. (h) Kovacic, V.; Hirsch, J.; Heerma, W. *Rapid Commun. Mass Spectrom.* **1997**, 11, 1353.

(6) (a) Mulrone, B.; Traeger, J. C.; Stone, B. A. *J. Mass Spectrom.* **1995**, 30, 1277. (b) Smith, G.; Leary, J. A. *J. Am. Soc. Mass Spectrom.* **1996**, 7, 953.

(7) (a) Puzo, G.; Fournié, J.-J.; Promé, J.-C. *Anal. Chem.* **1985**, 57, 892. (b) Puzo, G.; Promé, J.-C.; Fournié, J.-J. *Carbohydr. Res.* **1985**, 140, 131.

(8) (a) Smith, G.; Leary, J. A. *J. Am. Chem. Soc.* **1996**, 118, 3293. (b) Smith, G.; Pedersen, S. F.; Leary, J. A. *J. Org. Chem.* **1997**, 62, 2152.

(9) Bott, G.; Ogden, S.; Leary, J. A. *Rapid Commun. Mass Spectrom.* **1990**, 4, 341.

were obtained using an 8-kV accelerating voltage. The precursor ion was transmitted into the second field-free region and allowed to undergo unimolecular decomposition at a pressure of  $1 \times 10^{-8}$  Torr (no collision gas was added). The MIKES cell was at ground potential. The product ion spectra were generated by scanning the ESA while setting the magnet to pass only the mass of the precursor ion. The product ion spectra resulted from the signal averaging of 20 scans at a scan rate of 12 s/scan.

The FAB-Q-MIKES<sup>3</sup> and *m/z*-deconvoluted MIKES<sup>10</sup> studies were performed in a manner similar to the FAB-MIKES studies. However, the quadrupole mass analyzer was linked to the scanning of the ESA for the Q-MIKE spectra or was fixed to transmit only ions of a given mass-to-charge ratio for the *m/z*-deconvoluted MIKE spectra. Ions exiting the ESA were decelerated from 8 keV to 20 eV prior to transmission into the octapole collision cell. The octapole collision cell was used only to focus the ions into the final quadrupole and was operated at a pressure of  $1 \times 10^{-8}$  Torr (no collision gas was added). The resolution of the quadrupole was set to achieve unit mass resolution at the desired mass-to-charge ratio. Because of the significant decrease in sensitivity following transmission of the ions through the octapole and quadrupole, only partial *m/z* ranges (Q-MIKES) or kinetic energy ranges (*m/z*-deconvoluted MIKES) were obtained, with scan rates of 2 s/scan. Sufficient scan numbers (typically less than 500 for the labeled D-glucose complexes and ca. 2000 for the labeled D-mannose complexes) were signal-averaged to achieve a satisfactory S/N. Fresh sample aliquots were added to the probe tip after every 200 scans.

**Kinetic Energy Release Determination.** The KER values were calculated according to the equation below<sup>11</sup>

$$\text{KER} = \frac{y^2 m_1^2 E (\Delta E)^2}{16 m_2 m_3 (E)} \quad (1)$$

where  $m_1$  is the mass of the precursor ion,  $m_2$  is the mass of the product ion,  $m_3$  is the mass of the neutral loss,  $y$  is the charge of the product ion;  $E$  is the accelerating voltage (8000 kV),  $\Delta E = [\Delta E_{50\%}^2 - \Delta E_{(m_1)^2}]^{1/2}$ ,  $\Delta E_{50\%}^2$  is the width (in volts) of the product ion peak at half-height, and  $\Delta E_{(m_1)^2}$  is the width (in volts) of the precursor ion peak at half-height. All half-height widths were measured from the signal-averaged product ion spectra. To avoid overestimation of  $\Delta E_{(m_1)^2}$ , the precursor ion peak was not allowed to saturate the detector.

All MIKE spectra underwent smoothing and background subtraction prior to KER determination. Because of the dependence of the KER values upon the accurate measurement of peak widths and heights, alterations to the peak shape resulting from data processing was avoided. To ensure that excessive peak shape deformation did not occur, all processed data were carefully compared to the raw data.

Reported KER values result from the averaging of seven different measurements obtained under identical experimental conditions. Standard deviations were calculated for the mean KER values to determine the precision with which the measurements were obtained.

**High-Resolution Mass Measurements.** High-resolution FAB/MS was performed on precursor ions to check for isobaric interferences. Accurate mass measurements were made at a resolution of 1:20 000 by peak matching the *m/z* 293, 367, or 529 ion against internal standards PEG (*m/z* 283.1757), PEG(*m/z* 371.2281), or leucine enkephalin (*m/z* 556.2771), respectively.

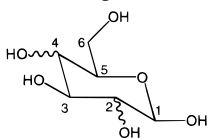
**Synthesis and FAB-MS Analysis.** Labeled and unlabeled Ni(II) *N*-glycoside complexes were synthesized using a microscaled adaptation of that previously published by Yano et al.<sup>12</sup> Briefly, 3 mg of Ni(DAP)<sub>3</sub>·2Cl<sup>-</sup>·2H<sub>2</sub>O and 4 mg of a D-aldohehexose were dissolved in

(10) (a) Alexander, A. J.; Thibault, P.; Guevremont, R.; Boyd, R. K. *Rapid Commun. Mass Spectrom.* **1988**, *2*, 79. (b) Ballard, K. D.; Gaskell, S. J. *J. Am. Soc. Mass Spectrom.* **1992**, *3*, 644.

(11) Cooks, R. G.; Beynon, J. H.; Caprioli, R. M.; Lester, G. R. *Metastable Ions*; Elsevier Scientific Publishing Co.: New York, 1973.

(12) (a) Shioi, H.; Yano, S.; Toriumi, K.; Ito, T.; Yoshikawa, S. *J. Chem. Soc., Chem. Commun.* **1983**, 5, 201. (b) Yano, S. *Coord. Chem. Rev.* **1988**, *92*, 113. (c) Yano, S.; Sakai, Y.; Toriumi, K.; Ito, T.; Ito, H.; Yoshikawa, S. *Inorg. Chem.* **1985**, *24*, 498. (d) Yano, S.; Kato, M.; Shioi, H.; Takahashi, T.; Tsubomura, T.; Toriumi, K.; Ito, T.; Hidai, M.; Yoshikawa, S. *J. Chem. Soc., Dalton Trans.* **1993**, 1699.

**Table 1.** Ring Substituent Configuration of D-Aldohexoses



monosaccharide	C-2 -OH	C-4 -OH
D-glucose	equatorial	equatorial
D-mannose	axial	equatorial
D-galactose	equatorial	axial
D-talose	axial	axial

200  $\mu$ L of methanol, yielding final concentrations of 0.04 and 0.12 M, respectively. The initially purple solutions yielded blue solutions following refluxing at 80  $^{\circ}$ C for 20 min. All reaction mixtures were kept at ca. 5  $^{\circ}$ C until used. No purification was performed prior to analysis. Authentic, purified samples of the octahedral D-glucose and D-mannose complexes were obtained from the laboratory of Professor Yano and were prepared as described in ref 12.

Solutions for FAB-MS were prepared by mixing 10  $\mu$ L of the crude Ni-*N*-glycoside reaction mixture (ca. 0.04 M) with 5  $\mu$ L of glycerol as matrix compound. Final concentration of all nickel-containing complexes was ca. 0.02 M. Approximately 1.5  $\mu$ L of the sample mixture was deposited onto the FAB probe tip. The sample was ionized with 20 kV Cs ions at a current of ca. 1.0  $\mu$ A.

**Computational Studies.** A series of 35 conformers were generated from a starting geometry by rotating around the C5-C6 bond and all C-OH bonds. The limited number of conformers was chosen using a Monte Carlo-based conformer generation package, implemented on Spartan 4.1.1.<sup>13</sup> All torsions in the resulting conformers were minimized using the Sybyl force field<sup>14</sup> in the molecular mechanics module of SPARTAN 4.1.1. The conformer possessing the lowest strain energy was chosen for further geometry optimization using density functional calculations.

The local spin density method, as implemented on SPARTAN 4.1.1, was used for all density functional calculations. Direct SCF and a medium mesh were used. The initial geometry optimization was performed using the DN basis set. This basis set is a numerical split-valence basis set that does not include polarization effects on any atoms. The resulting structure underwent further geometry minimization using the DN\*\* basis set (numerical split-valence basis set that includes polarization effects on all atoms).

**Chemicals and Materials.** D-Glucose, D-glucose-2-<sup>13</sup>C (99% <sup>13</sup>C), and D-mannose were obtained from Aldrich Chemical Co. (Milwaukee, WI). D-Galactose and D-talose were obtained from Sigma Chemical Co. (St. Louis, MO). D-Glucose-6-<sup>2</sup>H<sub>2</sub> (99% D) was obtained from Cambridge Isotope Laboratories (Andover, MA). D-Glucose-3-<sup>13</sup>C (99% <sup>13</sup>C), D-glucose-4-<sup>13</sup>C (99% <sup>13</sup>C), D-glucose-1-<sup>2</sup>H (98% D), D-mannose-6-<sup>2</sup>H<sub>2</sub> (98% D), D-mannose-3-<sup>13</sup>C (99% <sup>13</sup>C), and D-mannose-4-<sup>13</sup>C (98% <sup>13</sup>C) were obtained from Omicron Biochemical Co. (South Bend, IN). ACS grade methanol was purchased from Fisher Chemical Co. (Fairborn, NJ). Glycerol was purchased from Mallinckrodt, Inc. (Paris, KY). All materials were used as received without further purification.

## Results and Discussion

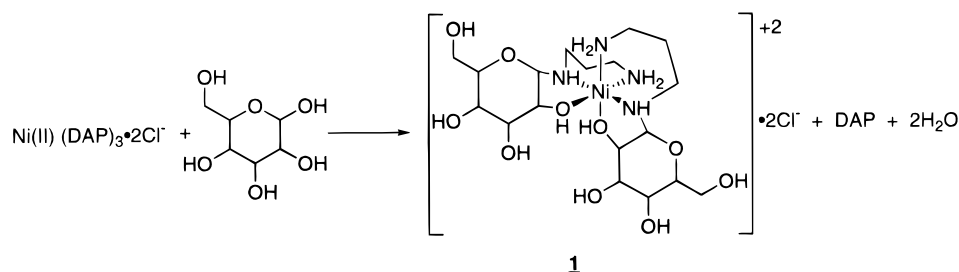
Nickel(II) *N*-glycoside complexes were synthesized using four diastereomeric D-aldohehexoses. Table 1 lists the orientations (equatorial or axial) of all ring substituents, assuming the monosaccharides occupy the energetically favorable <sup>4</sup>C<sub>1</sub> chair conformation.<sup>15</sup> Upon completion, such reactions are expected to yield complexes of the type Ni(NH<sub>2</sub>(CH<sub>2</sub>)<sub>3</sub>NH/(monosaccharide-H<sub>2</sub>O))<sub>2</sub>·2Cl<sup>-</sup> (**1**) (Scheme 1). Each neutral *N*-glycoside unit functions as a tridentate ligand where the monosaccharide

(13) SPARTAN version 4.1.1, Wavefunction, Inc., Irvine, CA. 92715.

(14) Clark, M.; Cramer, R. D., III; van Opdenbosch, N. J. *Comput. Chem.* **1989**, *10*, 982.

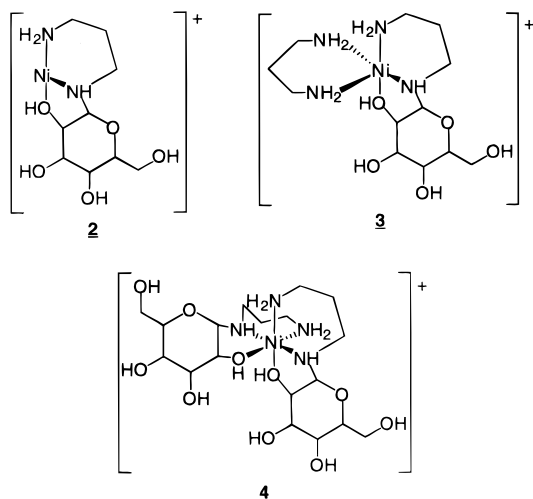
(15) (a) Jeffrey, G. A.; Yates, J. H. *Carbohydr. Res.* **1979**, *74*, 319. (b) Dowd, M. K.; French, A. D.; Reilly, P. J. *Carbohydr. Res.* **1994**, *264*, 1.

## Scheme 1



C-2 hydroxyl substituent and both amine nitrogens coordinate to the central nickel.<sup>12</sup>

The crude products from all four reactions were analyzed by FAB-MS. Figure 1 is the low-resolution mass spectrum obtained from the D-glucose reaction. The low-resolution mass spectra of the other monosaccharide reactions were qualitatively similar. A prominent series of singly charged ions ( $m/z$  293, 367, and 529) resulted from the deprotonation of various Ni(II) complexes. These deprotonated ions were assigned to tricoordinate (2), pentacoordinate (3), and octahedrally coordinated (4)



complexes, respectively. Additionally, an intense ion at  $m/z$  237, assigned to the protonated, metal-free *N*-glycoside ligand, is present.

High-resolution mass measurements were performed on various ions from the D-glucose reaction mixture in order to confirm the molecular assignment and rule out the presence of

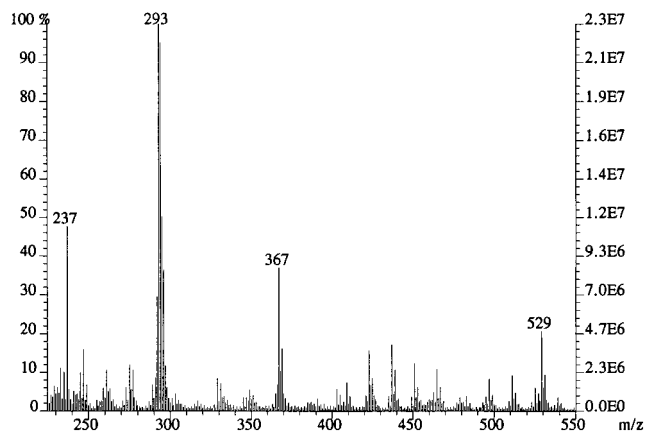


**Figure 1.** FAB mass spectrum of Ni(II)(NH<sub>2</sub>(CH<sub>2</sub>)<sub>3</sub>NH<sub>2</sub>)<sub>3</sub>·2Cl<sup>-</sup>/D-glucose reaction mixture with glycerol matrix.

**Table 2.** High-Resolution Mass Measurements of Ions from Crude Glucose Reaction Mixture

ion	experimental mass	theoretical mass	$\Delta$ (mmu)	composition
2	293.0645	293.0647	0.2	C <sub>9</sub> H <sub>19</sub> N <sub>2</sub> O <sub>5</sub> Ni
3	367.1491	367.1491	0.0	C <sub>12</sub> H <sub>29</sub> N <sub>4</sub> O <sub>5</sub> Ni
4	529.2026	529.2020	-0.6	C <sub>18</sub> H <sub>39</sub> N <sub>4</sub> O <sub>10</sub> Ni

**Table 3.** Product Ions Observed in Unimolecular MIKE Spectra of  $m/z$  293 Precursor Ion (2) from All Monosaccharide Reaction Mixtures (M = Structure 2)<sup>a</sup>

$m/z$	neutral loss (Da)	ion composition
275	18	M-H <sub>2</sub> O
263	30	M-CH <sub>2</sub> O
257	36	M-2H <sub>2</sub> O
245 <sup>a</sup>	48	M-(CH <sub>2</sub> O + H <sub>2</sub> O)
233 <sup>a</sup>	60	M-C <sub>2</sub> H <sub>4</sub> O <sub>2</sub>
203	90	M-C <sub>3</sub> H <sub>6</sub> O <sub>3</sub>
173	120	M-C <sub>4</sub> H <sub>8</sub> O <sub>4</sub>

<sup>a</sup> Relative intensities of the  $m/z$  245 and 233 product ions were <20% of the base product ion ( $m/z$  263) for the mannose and talose complexes.

isobaric interferences. Assignments of the  $m/z$  293, 367, and 529 ions are supported by the high-resolution measurements (Table 2).

The  $m/z$  293 ion generated for each of the four monosaccharide complexes was transmitted into the MIKES cell and allowed to undergo unimolecular dissociation. The MIKE spectrum of the  $m/z$  293 precursor ion from the D-glucose reaction has been published previously.<sup>8a</sup> Similar product ions were observed for all four monosaccharide complexes (Table 3). However, the intensities of the  $m/z$  245 and 233 product ions were very weak in the spectra of the D-mannose and D-talose complexes relative to that observed in the MIKE spectra of the D-glucose and D-galactose complexes.<sup>8a</sup> Several product ions ( $m/z$  233, 203, and 173) are consistent with various cross-ring cleavages in the carbohydrate moiety of the precursor ion.<sup>5b-c,5f,6b,16</sup> Additionally, narrow peaks were observed at  $m/z$  (apparent) 234 and 235. The relative intensities of these peaks were variable from sample to sample and may be attributed to artifacts from the dissociation of ions in the field-free region prior to the magnetic sector. Such artifacts are commonly observed in MIKE spectra<sup>10a,17</sup> and details of these artifacts are discussed below. Product ions resulting from bond cleavages in the diaminopropane portion of the *N*-glycoside ligand were not detected.

The average KER associated with the dissociation of the  $m/z$  293 precursor ion to the  $m/z$  233 product ion was determined

(16) Cerny, R. L.; Tomer, K. B.; Gross, M. L. *Org. Mass. Spectrom.* **1986**, *21*, 655.

(17) (a) Schaldach, B.; Grutzmacher, H.-F. *Org. Mass Spectrom.* **1980**, *15*, 166. (b) Ast, T.; Bozorgzadeh, M. H.; Wiebers, J. L.; Beynon, J. H.; Brenton, A. G. *Org. Mass Spectrom.* **1979**, *14*, 313.

(18) (a) Holmes, J. L. *Org. Mass Spectrom.* **1985**, *20*, 169. (b) Cerda, B. A.; Hoyau, S.; Ohanessian, G.; Wesdemiotis, C. *J. Am. Chem. Soc.* **1998**, *120*, 2437.

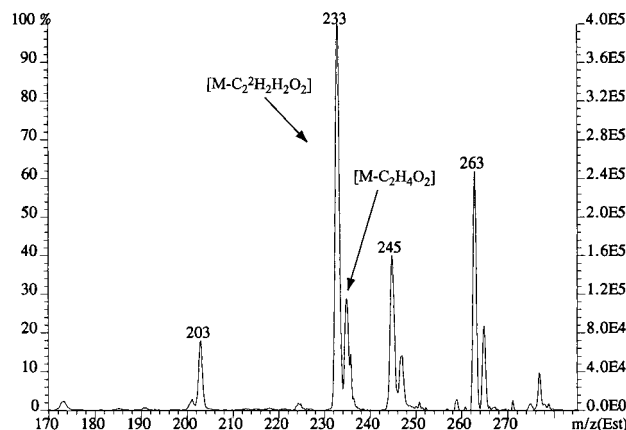


**Figure 2.** MIKE spectrum of  $m/z$  295 precursor ion from D-glucose-6- $^2\text{H}_2$  reaction mixture.

from the peak width at half-height for each of the four monosaccharide complexes as described in the Experimental Section. As was reported previously,<sup>8a</sup> the KER values associated with this dissociation were ca.  $30 \pm 3$  meV for complexes possessing a monosaccharide with an equatorial C-2 hydroxyl group (D-glucose, D-galactose), while those possessing an axial C-2 hydroxyl substituent displayed statistically significant differences in the KER values of ca.  $9 \pm 2$  meV. Dependence upon the C-4 substituent configuration was not apparent. Given the fact that these values are so low and that previously published data indicated that no reverse activation barriers are observed when the KER value is below 25 meV,<sup>18</sup> it is reasonable to assume that none exists for these systems as well. The value of 30 meV is very close to the upper limit, and therefore it cannot be conclusively assumed that there is no reverse activation barrier for the D-glucose and D-galactose complexes. The MIKE spectra and the KER results suggest that a single structural feature, an axial or equatorial orientation of the C-2 hydroxyl substituent, greatly affects the dissociation mechanisms of the deprotonated tricoordinate complexes. However, the origins of these phenomena were not readily

apparent. To address these issues and gain greater insight into the dissociation mechanisms of the Ni(II) *N*-glycoside complexes, isotopic labeling studies and DFT calculations were investigated.

MIKE spectra of the  $m/z$  293 precursor ion generated from authentic purified samples of the octahedral Ni(II) *N*-glycoside complexes (see Experimental Section) were identical to the spectra obtained from the reaction mixtures. The corresponding average KER values obtained using the authentic purified Ni(II) *N*-glycoside complexes were within the experimental error of the values obtained when analyzing the crude reaction mixtures of the same complexes.

**Isotopic Labeling Experiments.** Isotopically labeled Ni(II) *N*-glycoside complexes were synthesized to determine which carbons were present in the 60 Da neutral loss. A series of isotopically labeled D-glucose and D-mannose complexes were thus synthesized using a series of differently labeled monosaccharides: D-glucose-1- $^2\text{H}$ , D-glucose-2- $^{13}\text{C}$ , D-glucose-3- $^{13}\text{C}$ , D-glucose-4- $^{13}\text{C}$ , D-glucose-6- $^2\text{H}_2$ , D-mannose-3- $^{13}\text{C}$ , D-mannose-4- $^{13}\text{C}$ , and D-mannose-6- $^2\text{H}_2$ . Prominent ions at  $m/z$  295 observed in the low-resolution mass spectra of the D-glucose-6- $^2\text{H}_2$  and D-mannose-6- $^2\text{H}_2$  reaction mixtures were assigned to **2** possessing two deuterium atoms at C-6 of the monosaccharide moiety. Low resolution mass spectra of each of the D-glucose-1- $^2\text{H}$ , D-glucose-2- $^{13}\text{C}$ , D-glucose-3- $^{13}\text{C}$ , D-glucose-4- $^{13}\text{C}$ , D-mannose-3- $^{13}\text{C}$ , and D-mannose-4- $^{13}\text{C}$  reaction mixtures displayed prominent ions at  $m/z$  294. These ions are consistent with the incorporation of a single isotopically labeled atom ( $^2\text{H}$  or  $^{13}\text{C}$ ) into **2** at the corresponding positions of the monosaccharide moiety.

The MIKE spectrum of the  $m/z$  295 precursor ion from the D-glucose-6- $^2\text{H}_2$  reaction mixture is shown in Figure 2. Product ions were observed at  $m/z$  235 and 233 (neutral losses of 60 and 62 Da, respectively). The  $m/z$  235 product ion is consistent with an unlabeled  $\text{C}_2\text{H}_4\text{O}_2$  neutral loss, while the  $m/z$  233 product ion corresponds to a similar neutral loss containing C-6 and both deuterium atoms ( $\text{C}_2^2\text{H}_2\text{H}_2\text{O}_2$ ). It is apparent that at least two dissociation mechanisms, distinguished by the ultimate

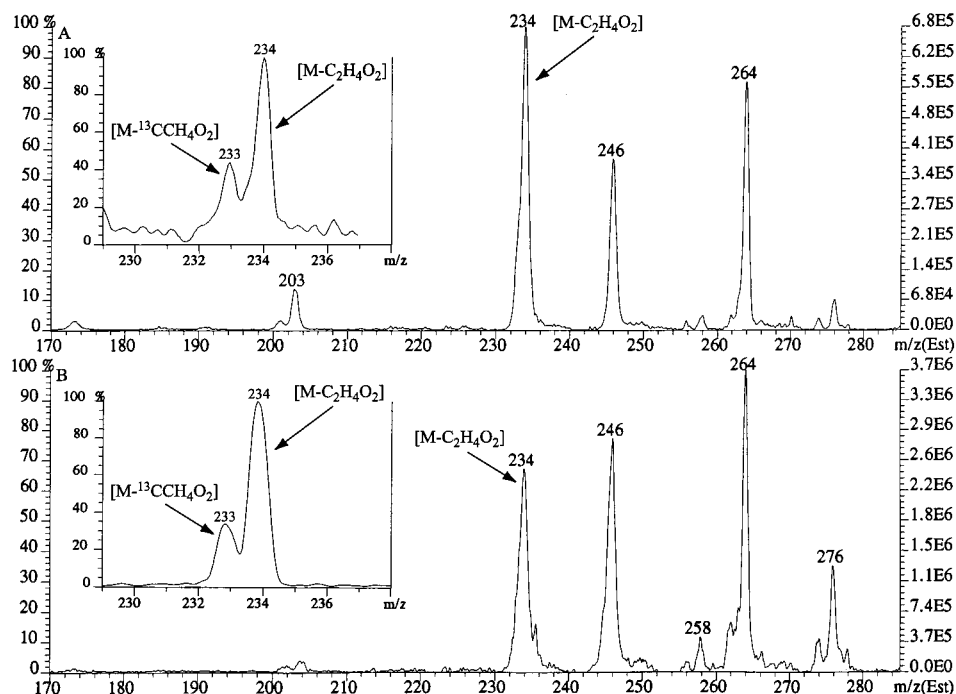


**Figure 3.** (A) MIKE spectrum of  $m/z$  294 precursor ion from D-glucose-4- $^{13}\text{C}$  reaction mixture. Inset: Partial Q-MIKE spectrum of same precursor ion. (B) MIKE spectrum of  $m/z$  294 precursor ion from D-glucose-3- $^{13}\text{C}$  reaction mixture. Inset: Partial Q-MIKE spectrum of same precursor ion.

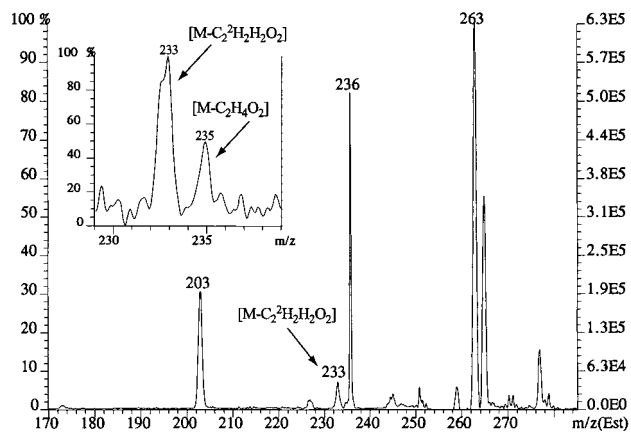


**Figure 4.** MIKE spectrum of  $m/z$  295 precursor ion from D-mannose-6- $^2\text{H}_2$  reaction mixture. Inset: Partial Q-MIKE spectrum of same precursor ion.

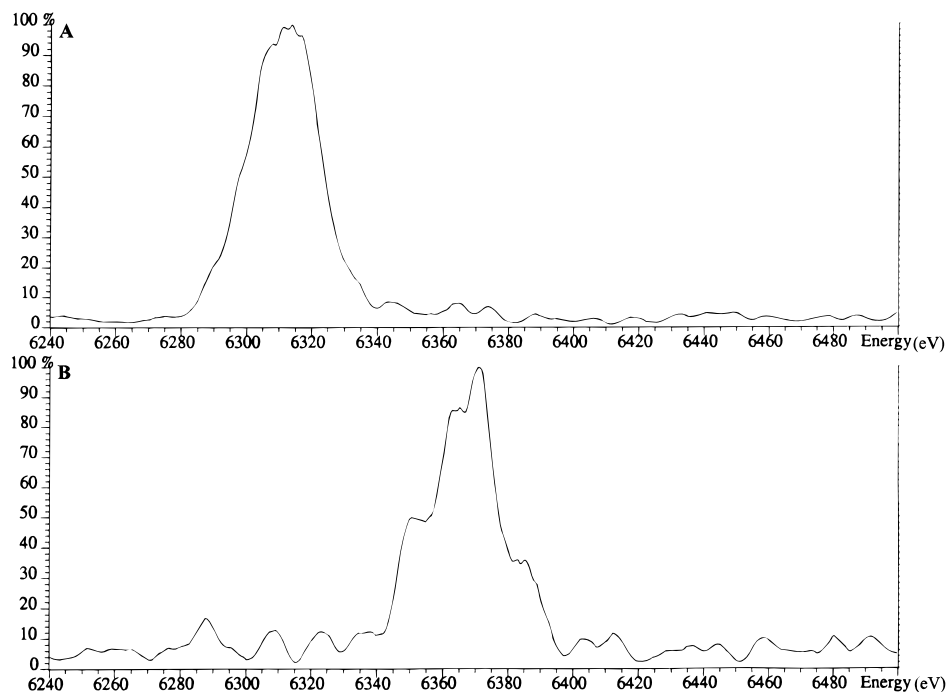
retention or loss of C-6 from the product ions, were observed. Because the resulting neutral losses and product ions have the same molecular formula in the unlabeled complex, these product ions generated via different pathways were indistinguishable in the previously published spectrum of the  $m/z$  293 precursor ion.<sup>8a</sup>

Figure 3A and B are the MIKE spectra of the  $m/z$  294 precursor ions from the D-glucose-4- $^{13}\text{C}$  and D-glucose-3- $^{13}\text{C}$  reaction mixtures, respectively. Product ions observed at  $m/z$  234 (neutral losses of 60) in both spectra are consistent with retention in the product ions of the labeled C-3 or C-4 atoms following losses of unlabeled  $\text{C}_2\text{H}_4\text{O}_2$  from the precursor ions.

Closer inspections of the peak shapes of the  $m/z$  234 product ions in Figure 3A and B revealed shoulders on the low mass sides of these peaks. Such shoulders could represent product ions at  $m/z$  233 resulting from  $^{13}\text{C}$ -labeled  $\text{C}_2\text{H}_4\text{O}_2$  neutral losses from the precursor ions. However, because KER peak broadening lowers the product ion resolution of MIKE spectra, it was impossible to resolve product ions having a 1 Da difference.

The insets in Figure 3A and B are partial Q-MIKES spectra obtained by linking the scanning of the ESA and the quadrupole mass analyzer<sup>3</sup>. Greater product ion resolution is achieved using this linked scanning technique as a result of the insensitivity of the quadrupole mass analyzer to the kinetic energy of the ions. The insets display a weak  $m/z$  233 product in addition to the more intense  $m/z$  234 product ion for both the D-glucose-4- $^{13}\text{C}$  and D-glucose-3- $^{13}\text{C}$  complexes. In contrast, MIKE spectra of the  $m/z$  294 precursor from the D-glucose-2- $^{13}\text{C}$  and D-glucose-1- $^2\text{H}$  reaction mixtures (data not shown) displayed a product ion at  $m/z$  234 with no apparent shoulders. Thus, all relevant dissociation pathways appeared to result in retention of the C-2 and C-1 in the product ion.

Figure 4 is the MIKE spectrum of the  $m/z$  295 precursor ion from the D-mannose-6- $^2\text{H}_2$  reaction mixture. A product ion at  $m/z$  233 (neutral loss of 62) is consistent with loss of C-6 from the precursor ion. The narrow peak at  $m/z$  (apparent) 236 (kinetic energy = 6389 eV) was assigned to an artifactual protonated glycerol tetramer ( $m/z$  369) resulting from the dissociation of a protonated glycerol pentamer ( $m/z$  461) in the first field-free region<sup>10a,17</sup> and is discussed in detail below. Because of the intense artifact ion at  $m/z$  (apparent) 236, it was impossible to conclusively determine the presence or absence of a product ion at  $m/z$  235. The Q-MIKE spectrum of the  $m/z$  295 precursor ion (inset, Figure 4) displays a weak  $m/z$  235 product ion in addition to the  $m/z$  233 product ion. MIKE spectra of the D-mannose-3- $^{13}\text{C}$  and D-mannose-4- $^{13}\text{C}$  complexes (data not shown) were similar to those of the correspondingly labeled D-glucose complexes inasmuch as they were suggestive of multiple dissociation mechanisms leading to a neutral  $\text{C}_2\text{H}_4\text{O}_2$  loss. However, the quality of the Q-MIKE spectra of all of the labeled D-mannose complexes was marginal because of the low abundance of the relevant product ions. Concern arose as to the possibility of higher mass ions giving rise to artifacts in the Q-MIKE linked spectra, especially in light of the presence an ion at  $m/z$  (apparent) 236 in Figure 4, which is so close in



**Figure 5.** (A)  $m/z$  233 product ion from  $m/z$  295 precursor ion of D-mannose-6- $^2\text{H}_2$  complex; (B)  $m/z$  235 product ion from  $m/z$  295 precursor ion of D-mannose-6- $^2\text{H}_2$  complex. Detector gain settings were higher for B than for A.

apparent mass to the ion of interest. It was therefore decided to implement mass-to-charge ratio deconvoluted MIKES experiments.<sup>10</sup>

In the mass-to-charge ratio deconvoluted MIKES experiments, the quadrupole is electronically decoupled from the ESA, and the quadrupole is set to transmit only ions of a desired mass-to-charge ratio. The resulting spectrum is a kinetic energy spectrum of only the desired product ion. This particular scan function precludes detection of product ions whose precursors are greater in mass than the selected precursor but having lower kinetic energies: i.e., artifact ions from decompositions of higher mass ions occurring outside the MIKES cell are not recorded.

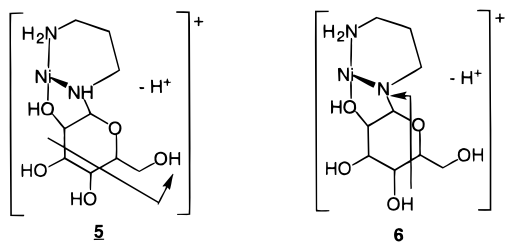
Figure 5A is the mass-to-charge ratio deconvoluted MIKES spectrum of the *m/z* 233 product ion generated from the *m/z* 295 precursor ion of the D-mannose-6-<sup>2</sup>H<sub>2</sub> reaction mixture. The kinetic energy of the *m/z* 233 product ion is centered at ca. 6315 eV. This agrees well with the predicted value

$$KE_{\text{lab}} = \left(\frac{233}{295}\right)8000 \text{ eV} = 6318 \text{ eV} \quad (2)$$

Thus, the *m/z* 233 product ion in Figure 5A is generated solely from the *m/z* 295 precursor; *m/z* 233 product ions generated from the dissociation of higher mass artifact ions would be observed at significantly lower kinetic energies and would not be detected in the mass-to-charge deconvoluted MIKES spectrum.

Figure 5B shows a similar mass-to-charge ratio deconvoluted MIKES spectrum of the *m/z* 235 product ion generated from the *m/z* 295 precursor ion of the D-mannose-6-<sup>2</sup>H<sub>2</sub> reaction mixture. A significant decrease in signal-to-noise was present in this spectrum due to the relatively low production efficiency of this product ion. Comparison of the observed kinetic energy of the product ion (ca. 6375 eV) with the predicted value (6373 eV) definitively indicates *m/z* 235 product ions were produced from the dissociation of the D-mannose-6-<sup>2</sup>H<sub>2</sub> complex.

Analysis of the results from the labeling studies allows for the postulation of some of the structural features of the different *m/z* 233 product ions. In the case of the D-glucose complex, no evidence was observed, suggesting the loss of either C-1 or C-2 from the monosaccharide ring. The absence of losses involving C-1 and C-2 are not surprising, considering that both atoms possess substituents directly coordinated to Ni(II), and are likely to be tightly bound to the metal center. Isotopic labeling experiments also show that C-3, C-4 or C-6 may be lost in the C<sub>2</sub>H<sub>4</sub>O<sub>2</sub> neutral loss. One likely product ion (**5**) can be inferred, resulting from cross-ring cleavages in the monosaccharide ring at bonds C-2/C-3 and C-4/C-5, with a subsequent loss of C-3 and C-4. Product ion **6** is also postulated where both C-6 and



C-5 are lost from the precursor ion. While experiments involving labeling of C-5 were not performed, one can reasonably deduce that this carbon center is also present in a C<sub>2</sub>H<sub>4</sub>O<sub>2</sub> loss. Formation of a C<sub>2</sub>H<sub>4</sub>O<sub>2</sub> loss possessing C-6, but not C-5, would require a considerable rearrangement in the ion structure along the dissociation pathway. Such extensive rearrangements are

likely to make the generation of product ions unfavorable. If **5** and **6** are the only two *m/z* 233 product ions, the fraction of the labeled and unlabeled product ions from the D-glucose-6-<sup>2</sup>H<sub>2</sub>, D-glucose-3-<sup>13</sup>C, and D-glucose-4-<sup>13</sup>C precursor ions suggests that **6** is the predominant product ion formed from the metastable precursor ions.

Extensive labeling experiments identical to those performed for the D-glucose complex were not performed for the D-mannose complex because of the limited number of labeled D-mannose compounds available; only three sites (C-6, C-4, and C-3) were specifically labeled. Similarities were still conclusively observed between the D-mannose and D-glucose complexes, suggesting that cross-ring cleavages in the monosaccharide moiety were occurring at similar sites as in **5** and **6** for both monosaccharide complexes. Isotopically labeled D-galactose and D-talose compounds were also not available. The invariability of the MIKES spectra and KER values with the changes in the configuration of the C-4 substituents suggests that the dissociation pathways of the D-glucose and D-mannose complexes are similar to those of the D-galactose and D-talose complexes, respectively. However, in the absence of more extensive mechanistic studies of the D-galactose and D-talose complexes, such comparisons cannot be confirmed.

**Computational Modeling Studies.** Although the structural features of the octahedral Ni(II) *N*-glycoside complexes have been investigated,<sup>12</sup> it would be unwise to assume that the coordination geometries of the ligand are identical in both the octahedral complex and the tricoordinate deprotonated complex. This is especially true, considering the unusual coordination state of Ni(II) in these complexes. Additionally, it is desirable to reach some conclusions about the relative stabilities of various sites of deprotonation in these complexes. Density functional theory calculations were used to predict the equilibrium geometries of different Ni(II) *N*-glycoside complexes possessing various sites of deprotonation. Starting coordination geometries were identical to those postulated for the octahedral complexes. Deprotonation sites at the C-2 hydroxyl group and the aminal nitrogen were chosen for two reasons. First, location of a negatively charged deprotonation site near the positively charged metal center is expected to stabilize the complex; both deprotonation sites are on substituents directly coordinated to Ni(II). Second, both deprotonation sites are on substituents of the monosaccharide ring. Such deprotonation sites may be expected to initiate charge-directed dissociation mechanisms involving the monosaccharide ring (e.g., cross-ring cleavages), whereas a deprotonation site on the primary amine is likely to be too distant to play a direct role in such dissociations.

Geometrically optimized structures of the D-glucose and D-mannose complexes following deprotonation at either the C-2 hydroxyl group or the secondary amine are shown in Figures 6 and 7, respectively. All structures were assumed to have a singlet ground electronic configuration, as is predicted for tricoordinate d<sup>8</sup> complexes.<sup>19</sup> At this time no attempts were made to predict the structures of either the D-talose or D-galactose complexes.

A predicted T-shaped coordination geometry of the *N*-glycoside ligand about Ni(II) is a consistent feature among all structures in Figures 6 and 7. Table 4 displays the bond lengths

(19) (a) Burdett, J. K. *Inorg. Chem.* **1975**, *14*, 375. (b) Burdett, J. K. *Inorg. Chem.* **1975**, *14*, 931. (c) Komiya, S.; Albright, T. A.; Hoffman, R.; Kochi, J. K. *J. Am. Chem. Soc.* **1976**, *98*, 7255. (d) Tatsumi, K.; Hoffman, R.; Yamamoto, A.; Stille, J. K. *Bull. Chem. Soc. Jpn.* **1981**, *54*, 1857. (e) Yamamoto, A.; Yamamoto, T.; Komiya, S.; Ozawa, F. *Pure Appl. Chem.* **1984**, *56*, 1621. (f) Fan, L.; Krzywicki, A.; Somogyvari, A.; Ziegler, T. *Inorg. Chem.* **1994**, *33*, 5287. (g) Margl, P.; Ziegler, T. *J. Am. Chem. Soc.* **1996**, *118*, 7337. (h) Deng, L.; Margl, P.; Ziegler, T. *J. Am. Chem. Soc.* **1997**, *119*, 1094.

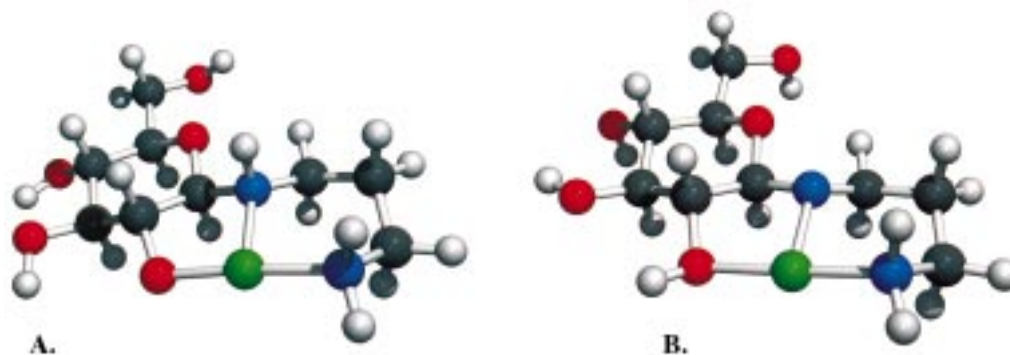


**Figure 6.** Structure of  $m/z$  293 Ni(DAP)/D-glucose complex. (A) Deprotonation site at C-2 hydroxyl group. (B) Deprotonation site at aminal site.

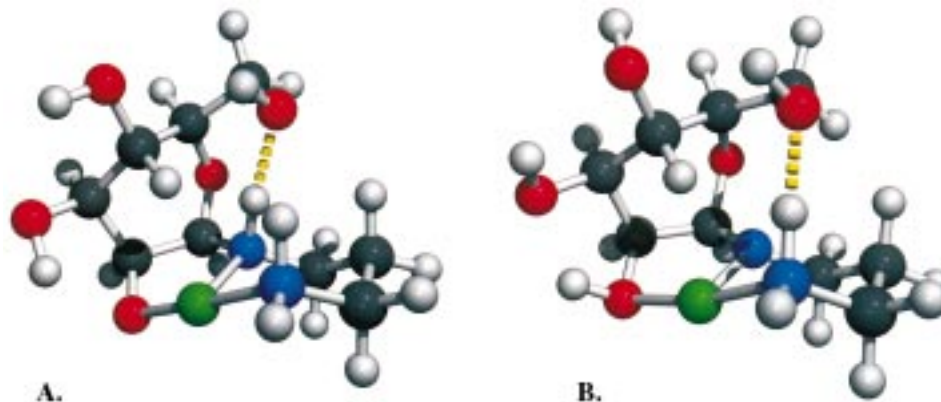


**Figure 7.** Structure of deprotonated, tricoordinate  $m/z$  293 Ni(DAP)/D-mannose complex. (A) Deprotonation site at C-2 hydroxyl group. (B) Deprotonation site at aminal site. The dashed yellow bars represent possible hydrogen-bonding interactions.

**Table 4.** Bond Distances and Bond Angles among Atoms Coordinated to Ni in Figures 5 and 6

monosacc.	bond length (Å)			bond angles (deg)		
	O–Ni	N1–Ni	N2–Ni	O–Ni–N1	N2–Ni–N1	O–Ni–N2
D-glucose (Figure 6A)	1.74	1.87	1.85	174.3	94.6	91.0
D-glucose (Figure 6B)	1.89	1.83	1.81	176.3	88.1	92.5
D-mannose (Figure 7A)	1.76	1.88	1.83	177.5	91.4	88.1
D-mannose (Figure 7B)	1.86	1.85	1.80	169.7	89.1	88.0

and angles among the atoms coordinated to the Ni(II) center. The bond angles indicate a nearly ideal square planar coordination geometry with a single vacant site. Alternate starting coordination geometries (trigonal planar and pyramidal) for the glucose complex also yielded a final T-shaped complex. Therefore, it is unlikely that the predicted coordination configuration about Ni(II) is an artifact of the starting geometry.

The predicted planar geometries of the deprotonated D-glucose *N*-glycoside ligands in Figure 6 are similar to that of the neutral ligand in the octahedral complex. The monosaccharide ring is predicted to maintain a  ${}^4C_1$  chair conformation. Consistent with this conformation, the dihedral angles between the coordinating substituents (the C-2 hydroxyl group and the aminal nitrogen) are 52.9 and 59.8° for the complexes possessing a deprotonation site at the hydroxyl group or the aminal, respectively.

Significant differences are present in the case of the deprotonated D-mannose *N*-glycoside ligands. The monosaccharide ring is predicted to occupy a twist-boat conformation, regardless of deprotonation site. The dihedral angles between the coordinating substituents (the C-2 hydroxyl group and the aminal nitrogen) are smaller than those observed in the D-glucose

complexes, being 30.7 and 30.8° in Figure 7A and B, respectively. This ring conformation also places the C-6 hydroxyl much closer to the diaminopropane portion of the ligand. Indeed, when the deprotonation site is on the C-2 hydroxyl group, the distance between the oxygen of the C-6 hydroxyl group and the proton of the secondary amine is predicted to be 1.77 Å. The corresponding OHN angle is 174.6°. Such orientations are indicative of an additional hydrogen bond in the D-mannose complex (Figure 7A). In the complex possessing a secondary amine deprotonation site, the distance between the oxygen of the C-6 hydroxyl group and one of the primary amine protons is 1.76 Å, with a corresponding OHN angle of 165.0°. Again, the presence of an additional hydrogen-bonding interaction is suggested in the D-mannose complex (Figure 7B).

The predicted relative stabilities of the different deprotonation sites are similar for the D-mannose and D-glucose complexes (Table 5). A deprotonation site on the C-2 hydroxyl group is favored by 13 kcal/mol (D-glucose complex) and 17 kcal/mol (D-mannose complex) over the secondary amine deprotonation site. A significant population of complexes possessing various deprotonation sites may be envisioned as being produced during

**Table 5.** Summary of Energy Results from Computational Study

	D-glucose	D-mannose
energy (hartree) C-2 hydroxyl deprot. site	-2339.108630	-2339.152104
rel. energy (kcal/mol)	-12.8	-16.5
energy (hartree) aminal deprot. site	-2339.088194	-2339.125731
rel. energy (kcal/mol)	0.0	0.0

the FAB-ionization process. Prior to becoming an isolated gaseous ion, the precursor ion will exist in a relatively high-pressure environment (i.e., the seldedge) for a finite period of time.<sup>20</sup> Under such higher pressure conditions, the precursor ion may undergo intermolecular proton transfer with species such as matrix molecules. The low barrier likely to be associated with the intermolecular proton transfers and the internal energies typically imparted during the FAB process (ca. 1 eV)<sup>21</sup> may allow for the formation of higher energy deprotonation sites on the precursor ion. Once the precursor ion has entered the low-pressure region of the analyzer, the mechanism for transferring the site of deprotonation is restricted to intramolecular proton transfers that are likely to possess significant barriers.

**Dissociation Mechanisms.** Direct evidence of the details of the multiple dissociation mechanisms, such as the reacting configuration of the precursor ions and the product ion structures, are few except for the knowledge of the presence or absence of various carbon centers in the product ions. Dissociation mechanisms can still be postulated with this limited information.

The postulated mechanism (Scheme 2) for the formation of **6** involves an initial deprotonation site on the aminal nitrogen (**7**). The predicted lowest energy structures of **7** for the D-glucose and D-mannose complexes are shown in Figures 6B and 7B, respectively. The internal energy typically imparted into a molecule during the FAB-ionization process<sup>21</sup> should allow for the formation of this higher energy structure (see above). An intermediate (**8**) possessing a secondary alkoxide site on the ligand may then be generated following the opening of the monosaccharide ring. One possible dissociation pathway leading from **8** may involve a concerted formation of a cyclobutane ring and a C<sub>2</sub>H<sub>4</sub>O<sub>2</sub> neutral loss containing C-5 and C-6 (**9**).

Another possible pathway from **8** could be the formation of an intermediate ion-dipole complex (**10**) possessing a carbanion at C-4, following heterolytic cleavage of the C-4/C-5  $\sigma$  bond. The generation of such ion-dipole complexes from simpler alkoxide anion systems, and their dissociation pathways have been well documented by Brauman<sup>22</sup> and Squires.<sup>23</sup> One likely pathway from **10** can result from the dissociation of the ion-dipole complex (Scheme 2). Such a dissociation of **10** will lead to the formation of a  $m/z$  233 product ion, **11**, with a resulting C<sub>2</sub>H<sub>4</sub>O<sub>2</sub> neutral loss containing C-5 and C-6. Such dissociation mechanisms have been observed from the ion-dipole complexes of primary and secondary alkoxides.<sup>23</sup> The ion-dipole complex must overcome only a single barrier due to the ion-dipole interaction energy to form **11**.<sup>22</sup> While further stabilizing rearrangements in **11** are possible, such processes occurring outside of the ion-dipole complex will not affect the observed KER values (i.e., a mechanism will not be present whereby the

internal energy of the isolated product ion is coupled to its kinetic energy).

Proton transfer within **10** may also occur, yielding an enolate-cation complex. Proton transfers within the ion-dipole complexes of simple alkoxides have been observed, producing another ion-dipole complex.<sup>22,23</sup> Such processes are especially favored when the ion in the original ion-dipole complex is a strong base. The large basicity of the carbanion at C-4 in **10** should make a proton-transfer feasible within the enolate-cation complex. The barrier to proton transfer within **10** will likely be similar for both the metal complex and the simple alkoxide anions. However, the energy required to separate the oppositely charged enolate and product ions will be considerably greater than that required to overcome the weaker ion-dipole interactions observed in the simpler alkoxide systems.

At least two product ion structures (**9** and **11**) are consistent with the isotopic labeling results, whereby C-5 and C-6 are present in a C<sub>2</sub>H<sub>4</sub>O<sub>2</sub> neutral loss following cross-ring cleavages in the monosaccharide ring. With the available data, it is impossible to conclusively identify the occurrence of one or both product ion structures. Additional MS<sup>3</sup> experiments are necessary to directly probe the structure of this product ion.

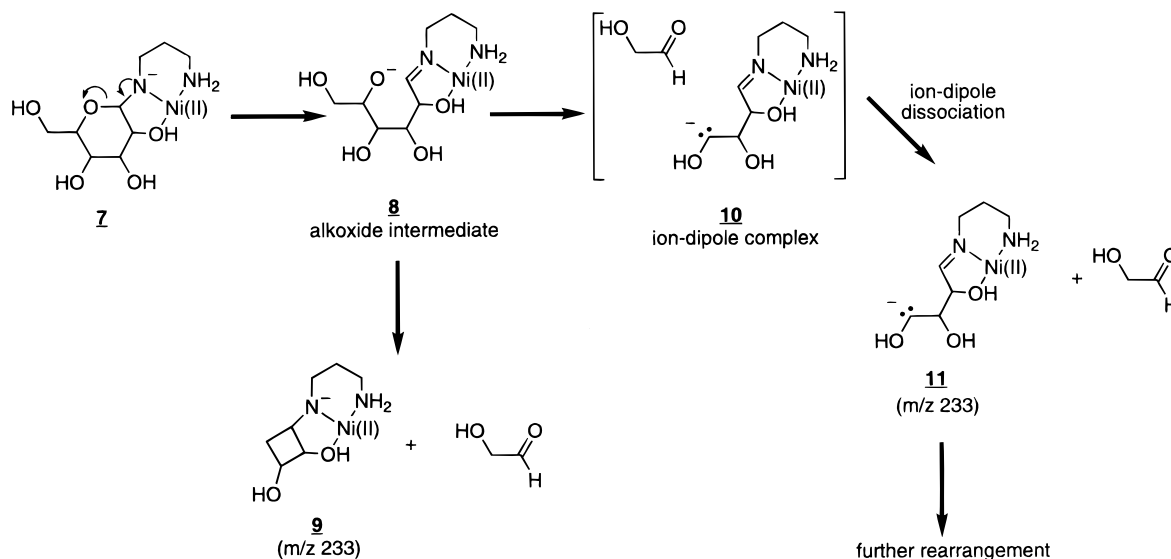
Comparisons of the predicted structure of **7** for the D-glucose and D-mannose complexes reveals a significant difference: the possible presence of an additional intramolecular hydrogen-bonding interaction between the C-6 hydroxyl group and a proton on the primary amine in the D-mannose complex (Figure 7B) but not in the D-glucose complex (Figure 6B). This additional interaction can greatly affect the dissociation energetics, and specifically the KER values, of the complexes possessing axial C-2 hydroxyl substituents. One may predict that the dissociation of the D-mannose ion-dipole complex **10** may require greater energies because the intramolecular hydrogen bonding forces must be overcome in addition to the ion-dipole forces. The corresponding intermediate **10** for the D-glucose complex need only overcome the ion-dipole interactions. Such a prediction is supported by the relatively low intensity of the  $m/z$  233 product ions for the D-mannose complex relative to that observed for the D-glucose complex.

Scheme 3 shows a postulated mechanism for the formation of the less abundant  $m/z$  233 product ion resulting from the cross-ring cleavages indicated in **5**. The initial site of deprotonation is located on the C-2 hydroxyl group, yielding a nickel-alkoxy complex (**12**). Evidence for such complexes has been previously observed.<sup>8b,24</sup> The predicted lowest energy structures for **12** of the D-glucose and D-mannose complexes are shown in Figures 6A and 7A, respectively. Comparison of the relative stabilities of various deprotonation sites, as predicted by the computational studies above, indicates that the C-2 hydroxyl group is a reasonable site of deprotonation. Following formation of the neutral loss, an intermediate (**13**) is generated. Subsequent rearrangements in **13** may be envisioned, such as those involving intramolecular nucleophilic additions (**14a**) or proton transfers (**14b**). Carbanions such as that postulated in **13** may be unstable. Previous studies have indicated that anions resulting from  $\alpha$ -deprotonation of ethers are less stable than their corresponding radicals<sup>25</sup> (e.g., the electron affinity of CH<sub>3</sub>OCH<sub>2</sub>• is ca. 0 kcal/mol). However, the presence of nearby electron-withdrawing groups, such as the  $\beta$ -hydroxyl substituent or the positively charged Ni(II) center, may stabilize **13**. Still, the formation of **13** may represent a fairly large barrier along the dissociation

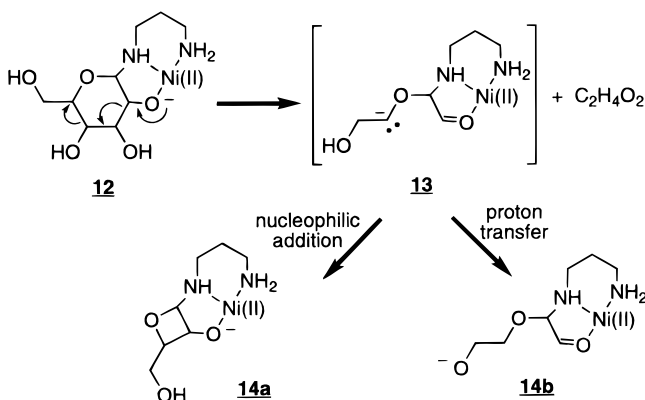
(20) Sunner, J. *Org. Mass Spectrom.* **1993**, *28*, 805.(21) Williams, D. H.; Naylor, S. *J. Chem. Soc., Chem. Commun.* **1987**, 1408.(22) (a) Tumas, W.; Foster, R. F.; Brauman, J. I.; *J. Am. Chem. Soc.* **1984**, *106*, 4053. (b) Tumas, W.; Foster, R. F.; Pellerite, M. J.; Brauman, J. I.; *J. Am. Chem. Soc.* **1987**, *109*, 961. (c) Tumas, W.; Foster, R. F.; Brauman, J. I. *J. Am. Chem. Soc.* **1988**, *110*, 2714.(23) Graul, S. T.; Squires, R. R. *J. Am. Chem. Soc.* **1990**, *112*, 2517.(24) Mehrotra, R. C. *Adv. Inorg. Chem. Radiochem.* **1983**, *26*, 269.(25) (a) DePuy, C. H.; Bierbaum, V. M.; Damrauer, R. *J. Am. Chem. Soc.* **1984**, *106*, 4051. (b) Waugh, R. J.; Hayes, R. N.; Eichinger, P. C.; Downard, K. M.; Bowie, J. H. *J. Am. Chem. Soc.* **1990**, *112*, 2537.



## Scheme 2

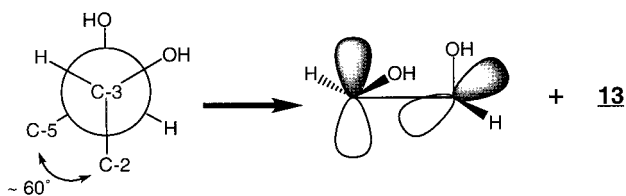


## Scheme 3



pathway. Although the postulated mechanism in Scheme 3 is not ideal, it is difficult to envision alternate pathways to **5** with fewer carbanionic intermediates and one where C-3 and C-4 are both present in the C<sub>2</sub>H<sub>4</sub>O<sub>2</sub> neutral loss.

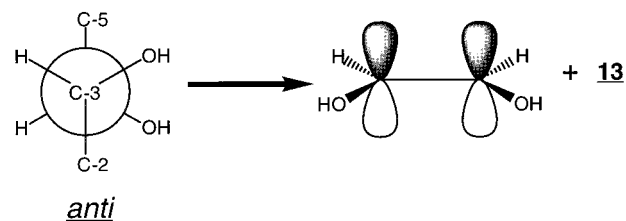
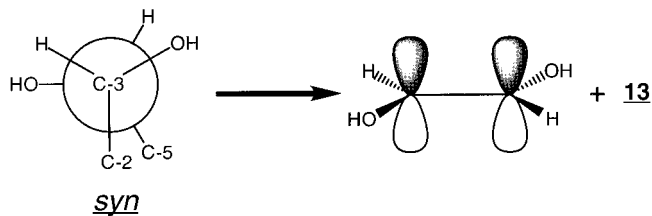
The postulated mechanism in Scheme 3 includes the formation of a  $m/z$  233 product ion via a single concerted step following the loss of HOHC=CHOH. Because the formation of a new C–C  $\pi$  bond is predicted in the neutral loss, this concerted process will be energetically feasible only if certain stereochemical features in the precursor ion structure are present. The major feature involves the relative orientations of the reacting configuration orbitals from which the C–C  $\pi$  bond is formed. For all of the monosaccharide complexes, the relevant orbitals are involved in the formation of the C-2/C-3 and C-4/C-5  $\sigma$  bonds in the precursor ions. Shown below is a Newman projection down the C-3/C-4 bond axis, applicable to the predicted lowest energy structures of **12** for both D-glucose and D-mannose complexes, illustrating the relative orientations of the relevant C–C  $\sigma$  bonds



The dihedral angle between the C-2/C-3 and C-4/C-5  $\sigma$  bonds

(and constituent orbitals) are predicted to be 56.3 and 66.2° in **12** for the D-glucose and D-mannose complexes, respectively. Therefore, the orbitals which should form the C–C  $\pi$  bond in the neutral loss will initially be nearly orthogonal to each other, as shown above, following the concerted dissociation in Scheme 3. Since the average bond energy of a C–C  $\pi$  bond is approximately 60 kcal/mol,<sup>26</sup> it is likely that a concerted loss of C<sub>2</sub>H<sub>4</sub>O<sub>2</sub> from the predicted lowest energy structures of **12** may not be energetically feasible. However, if low-energy conformational changes (i.e., <60 kcal/mol) in the precursor ion allow for the formation of a lower energy neutral loss (i.e., one possessing a full C–C  $\pi$  bond), the mechanism in Scheme 3 may become energetically feasible.

One may identify two orientations of the C-2/C-3 and C-4/C-5  $\sigma$  bonds which are capable of forming a full C–C  $\pi$  bond in the neutral loss during the concerted step in Scheme 3. These are syn (eclipsed C–C  $\sigma$  bonds) and anti orientations as shown below in the Newman projections down the C-3/C-4 bond axis of a monosaccharide ring



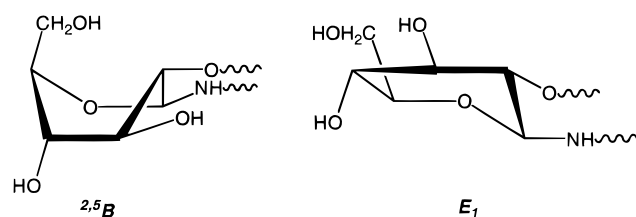
A six-membered ring is incapable of occupying such an anti geometry. Therefore, only those ring conformations possessing a syn geometry along the C-3/C-4 bond axis need be considered.

Many ring conformations of the monosaccharide in the D-glucose complex were assessed for the above-mentioned syn

(26) Weininger, S. J.; Stermitz, F. R. *Organic Chemistry*; Academic Press: Orlando, FL, 1984.

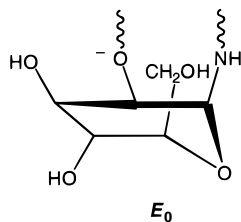
geometry, including all chair (C), boat (B), twist-boat, half-chair (H), skew (S), and envelope (E) conformers. Of these, only eight conformers were identified as having the desired syn orientation. They include four envelope ( ${}^{\circ}E$ ,  $E_0$ ,  $E_1$ , and  $E_2$ ), two-half-chairs ( ${}^1H_0$  and  ${}^1H_1$ ), and two boat conformers ( ${}^{2,5}B$  and  $B_{2,5}$ ). (See ref 15b for structural description of all conformers.) Six conformers could be discounted because they would significantly alter the coordination geometry of the ligand; the dihedral angle between the coordinating aminal nitrogen and the deprotonated C-2 hydroxyl group in **12** of the D-glucose complex would increase from the predicted  $53.1^\circ$ , to anywhere from  $90$  to  $180^\circ$ . Such changes in coordination geometry may possess significant barriers or lead to the formation of a ligand structure that is incapable of acting effectively as a tridentate ligand. These conformational changes are not likely to allow for an energetically feasible formation of the neutral  $C_2H_4O_2$  loss and **13**.

The remaining two conformers,  ${}^{2,5}B$  and  $E_1$ , are capable of maintaining a coordination geometry around the metal center identical to that predicted for the lowest energy structure in Figure 6A. The idealized structures of such ring conformations are shown below. Both conformers have been predicted to be



approximately 10 kcal/mol above the lowest energy  ${}^4C_1$  conformer in free  $\beta$ -D-glucose.<sup>15b</sup> The energy required for such conformational changes in the Ni(II) complex are likely to be similar to that predicted for free  $\beta$ -D-glucose since the portion of the ligand undergoing the structural change is removed from the site of direct metal–ligand interactions. One may then conclude that the D-glucose complex **12** may undergo low-energy conformational changes leading to a reacting configuration where the energy requirements are lowered for the generation of  $C_2H_4O_2$  containing C-3 and C-4. The dissociation mechanism shown in Scheme 3 may thus become a competitive process.

Methods similar to that used for the evaluation of potential conformational changes in the D-glucose complex **12** may also be used for the corresponding D-mannose complex. Again, the same set of eight conformers possesses the appropriate syn geometry around the C-3/C-4 bond axis. Only one conformer,  $E_0$ , is capable of preserving the coordination geometry of the ligand about the metal after the conformational change. The idealized structure of such a ring conformation is shown below



However, it is unclear how easily the transformation from the twist-boat to  $E_0$  can occur. First,  $E_0$  is a relatively high-energy conformer in free  $\beta$ -D-mannose, as it is predicted to be approximately 20 kcal/mol higher in energy than the  ${}^4C_1$  chair conformer.<sup>15</sup> While the monosaccharide ring in the D-mannose

ligand is predicted to be in the less stable twist-boat conformation, the twist-boat structure is typically only 5 kcal/mol less stable than the chair conformation in six-membered rings.<sup>26</sup> Thus, all other things considered equal, more energy is likely required for the conformational change in the D-mannose complex ( $\sim 15$  kcal/mol) than for the D-glucose complex ( $\sim 10$  kcal/mol). Second, the presence of an additional hydrogen-bonding interaction in the D-mannose complex may effect a less energetically favorable conformational change. Analysis of CPK models of **12** of the D-mannose complex reveals that the hydrogen bond between the C-6 hydroxyl group and the aminal nitrogen is difficult to maintain during and after the conformational change. If this hydrogen bond is weakened or broken, the energy requirements for this structural change will obviously increase. Therefore, it seems plausible that, for the D-mannose complex, more energy may be required to generate a reacting configuration from which a low energy form of  $C_2H_4O_2$  may be lost. It may then be inferred that the dissociation mechanism in Scheme 3 will be less competitive than that observed for the D-glucose complex. Indeed, the low intensity of such product ions in the MIKE spectra of the D-mannose complex supports these conclusions.

The postulated dissociation mechanisms in Schemes 2 and 3 suggest that the  $m/z$  233 product ion resulting from the loss of C-5 and C-6 is formed from a precursor ion possessing a deprotonation site that is higher in energy than that which leads to the formation of the  $m/z$  233 product ion resulting from the loss of C-3 and C-4. These implied features of Schemes 2 and 3 might appear to contradict the experimental evidence indicating that the formation of the  $m/z$  233 product ion resulting from the loss of C-5 and C-6 is the dominant of the two pathways. This apparent contradiction can be addressed by realizing that MIKE spectra reflect the dissociations of a precursor ion over a well-defined time span, as defined by the amount of time spent by the precursor ion within the MIKES cell. Thus, these product ion spectra may be accurately regarded as kinetic experiments. As such, the product ions and their relative intensities in the MIKE spectra will depend strongly upon the features of the potential energy surface (i.e., reaction barriers) along the relevant dissociation pathways. It is possible that a higher barrier (or barriers) leading to the loss of C-3 and C-4 will result in a lower yield of  $m/z$  233 product ions resulting from losses of C-3 and C-4, relative to that resulting from the loss of C-5 and C-6. This conclusion may still be valid even if the  $m/z$  293 precursor ion **12** is higher in energy than **7**. Unfortunately, it is unlikely that detailed, reliable information regarding the potential energy surface of such dissociation mechanisms can be obtained from the presented data to confirm such assumptions.

## Conclusions

Labeling experiments have shed much light upon the dissociation pathways of nickel/monosaccharide complexes. The labeling experiments conclusively show the presence of at least two isomeric product ions from the D-glucose and D-mannose complexes (and presumably the D-galactose and D-talose complexes) following cross-ring cleavages at different locations (**5** and **6**) of the monosaccharide ring. Additionally, the postulated dissociation mechanisms have implied the presence of multiple precursor ion structures for a given monosaccharide complex, differing in the site of deprotonation. The relative stabilities of several deprotonation sites, as predicted by DFT calculations, indicate that various precursor ion structures are

feasible under FAB conditions for the various Ni(II) *N*-glycoside complexes. Analysis of the stereochemical requirements of one of the dissociation pathways suggested that conformational changes in the precursor ion might allow some cross-ring cleavage mechanisms to become more energetically favorable. The presence of multiple dissociation pathways originating from potentially different reacting configurations and yielding different product ion structures does not allow for a simple interpretation of the average KER values of a given monosaccharide complex. Future analysis of the KER distributions may allow for a more complete analysis of these dissociation pathways.

The computational studies also predicted significant structural differences between the diastereomeric complexes, which possessed either axial or equatorial C-2 substituents, regardless of the site of deprotonation. These variations include additional intramolecular hydrogen-bonding interactions and different

monosaccharide ring conformations in the lowest energy structure of the D-glucose and D-mannose complexes. The presence of additional intraligand interactions and the concurrent conformational distortions in the ligand structures of complexes possessing axial C-2 -OH groups may drastically affect the energetics of all dissociation pathways observed for these complexes. Such structural variations may be reflected by the differences in the average KER previously reported.<sup>8a</sup>

**Acknowledgment.** The authors acknowledge NIH Grant No. GM47356 for their financial support. They would also like to thank Omicron Biochemical, Inc., for their generous donation of some of the labeled monosaccharide compounds and Professor Yano for his gracious donation of the purified Ni(DAP)/D-glucose and D-mannose samples.

JA9814319